Self-compression of millijoule 1.5 μm pulses

Oliver D. Mücke,[1,*] Skirmantas Ališauskas,[1,2] Aart J. Verhoef,[1] Audrius Pugžlys,[1] Andrius Baltuška,[1] Valerijus Smilgevičius,[2] Jonas Pocius,[3] Linas Giniūnas,[3] Romualdas Danielius,[3] and Nicolas Forget[4]

[1] *Photonics Institute, Vienna University of Technology, Gusshausstrasse 27-387, A-1040 Vienna, Austria*
[2] *Laser Research Center, Vilnius University, Saulėtekio av. 10, LT-10223 Vilnius, Lithuania*
[3] *Light Conversion Limited, P.O. Box 1485, Saulėtekio av. 10, LT-10223 Vilnius, Lithuania*
[4] *Fastlite, Bâtiment 403, Ecole Polytechnique, F-91128 Palaiseau, France*
**Corresponding author: oliver.muecke@tuwien.ac.at*

Received May 15, 2009; revised July 11, 2009; accepted July 13, 2009;
posted July 27, 2009 (Doc. ID 111454); published August 13, 2009

We demonstrate a four-stage optical parametric chirped-pulse amplification system that delivers carrier-envelope phase-stable ~1.5 μm pulses with energies up to 12.5 mJ before recompression. The system is based on a fusion of femtosecond diode-pumped solid-state Yb technology and a picosecond 100 mJ Nd:YAG pump laser. Pulses with 62 nm bandwidth are recompressed to a 74.4 fs duration close to the transform limit. To show the way toward a terawatt-peak-power single-cycle IR source, we demonstrate self-compression of 2.2 mJ pulses down to 19.8 fs duration in a single filament in argon with a 1.5 mJ output energy and 66% energy throughput.

OCIS codes: 320.7110, 190.4970.

Recently, optical parametric chirped-pulse amplification (OPCPA) has attracted much attention as a promising route toward intensity scaling of few-cycle laser pulses. Intense carrier-envelope phase (CEP)-stable few-cycle laser pulses have numerous intriguing applications in attosecond physics and high-field science [1]. In particular, high-energy few-cycle IR pulses [2–4] featuring high ponderomotive energy $U_p \propto \lambda^2 I$ at moderate intensity levels and a longer carrier wavelength λ have tremendous impact for many experiments. For example, high-U_p sources open the door to experimental investigation of the λ-scaling laws of strong-field physics [5–7] [electron kinetic energies $\propto\lambda^2$, high-harmonic generation (HHG) cutoff $\propto\lambda^2$, single-atom HHG efficiency $\propto\lambda^{-5.5}$, minimum attosecond pulse duration $\propto\lambda^{-1/2}$], and they would benefit laser-induced electron diffraction and permit time-resolved tomography of molecular dissociative states. Most importantly, phase-matched HHG driven by intense few-cycle IR pulses represents a promising route toward bright coherent sources in the soft and hard x-ray regions [8–10].

Parametric amplification of CEP-stable two-cycle IR seed pulses obtained from difference-frequency generation (DFG) to the energy level close to 1 mJ has been demonstrated [2,3]. However, the inherently low DFG seed energy causes a sizable superfluorescence background [2] that prevents further energy upscaling. By narrowing the bandwidth of an optical parametric amplifier (OPA), one can optimize the spectral brightness of the seed at the expense of the seed energy, achieve a more uniform saturation across the pulse spectrum, and minimize energy backconversion into the pump. In saturation, however, the parametrically amplified spectra exhibit steep slopes that lead to poor fidelity of the compressed pulses in the time domain.

Recently, Hauri *et al.* [11] demonstrated that filamentation of ~55 fs OPA pulses at 2 μm in a xenon cell allows the generation of self-compressed spectrally broadened 17 fs, 0.27 mJ pulses. The limited pulse energy available in that experiment implied the use of xenon as a noble gas with the highest nonlinearity. Detailed numerical investigations of self-compression of 2 μm laser filaments in gases with a moderate ionization potential I_p(<20 eV) [12] predicted a number of attractive features of femtosecond filamentation at longer wavelengths including higher filament energies, broader supercontinua with a flatter spectral phase, and the feasibility to reach single-cycle pulse durations in comparison with two- to three-cycle durations at visible wavelengths.

These fascinating numerical findings motivated us to explore the filamentation approach with pulses from a multimillijoule four-stage IR OPCPA (Fig. 1). The front end of the OPCPA is based on a femtosecond Yb:KGW diode-pumped solid-state (DPSS) master-oscillator power amplifier (MOPA) (Pharos, Light Conversion, Ltd.) and two stages of CEP-stable parametric preamplifiers [13]. Here we add two OPCPA boosters that allow us to reach pulse energies >10 mJ. Amplification stages 2–4 employ Type II KTP crystals ($\theta=45.5°$, $\varphi=0°$), which exhibit a relatively broad bandwidth around 1.5 μm [13,14].

The first significant advantage of using the femtosecond Yb front end is the ease of optical synchronization since both Yb and Nd regenerative amplifiers

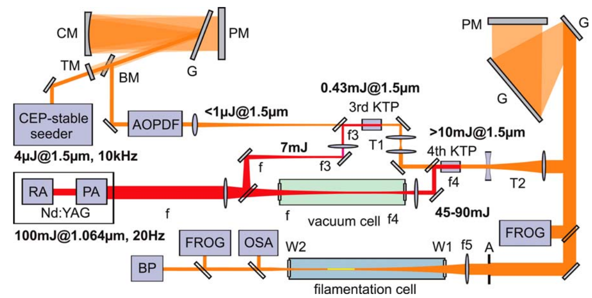

Fig. 1. (Color online) Scheme of the OPCPA power-amplification stages three and four: G, reflection grating; CM, curved mirror; PM, plane mirror; TM/BM, top/bottom mirror; AOPDF, acousto-optic programmable dispersive filter; RA, regenerative amplifier; PA, double-pass postamplifier; f, f3, f4, f5, lens focal lengths; T1, T2, telescopes; A, aperture; W1/W2, input/output windows; BP, beam profiler.

0146-9592/09/162498-3/$15.00

(RAs) at 1030 and 1064 nm, respectively, are simultaneously seeded from a single Yb master oscillator that emits 30 nm FWHM bandwidth pulses (not shown). To seed the Nd:YAG RA, we pick up unused 1064 nm light behind a transmission grating in the pulse stretcher of the Yb:KGW MOPA. The repetition rate of this MOPA, tunable within 1–100 kHz, was set at 10 kHz, i.e., at the 500th harmonic of the 20 Hz flashlamp-pumped 100 mJ Nd:YAG amplifier (Ekspla, Ltd.). In the Nd:YAG RA, an intracavity etalon is used to narrow the pulse bandwidth and keep the pulse duration safe for postamplification.

The CEP-stable 1.5 μm pulses from the front end are temporally stretched to ~40 ps using a grating-based stretcher and an IR high-resolution acousto-optic programmable dispersive filter (DAZZLER by Fastlite) [13] to optimize energy extraction from the 60 ps long Nd:YAG pump pulses. To guarantee a homogeneous pump profile free of hot spots, we relay image the 10 mm diameter crystal rod in the Nd:YAG power amplifier onto the 10-mm-thick KTP crystals in stages three and four. From the measured surface damage threshold of KTP for our pump pulses (21 GW/cm^2), we obtain a pump diameter of 2 mm for stage three and 3.1 mm for stage four. Relay imaging is achieved with three lenses with focal lengths of f=75 cm, f3=10 cm, and f4=35 cm. Because of the larger pump intensities in the fourth stage, the focus needs to be placed inside a vacuum cell to avoid a breakthrough in air. The 1.5 μm (seed) pulses are focused onto the third-stage KTP crystal with a 750 mm lens and imaged onto the fourth-stage KTP crystal with telescope T1. The (external) walk-off compensation angle between pump and seed beam is 2.1°. With this pumping geometry and 45–90 mJ pump pulses, we achieved up to 12.5 mJ signal pulses centered at 1.57 μm and a pump-signal conversion efficiency of ~22% in the final OPCPA stage. To avoid damage to the gold gratings in the OPCPA compressor, we expand the $1/e^2$ beam diameter of the fourth-stage output by a factor of 5 to 9.5 mm by means of Galilean beam expander T2.

The spectra of the seed and amplified signal pulses of the power-amplification stages are shown in Fig. 2. In principle, saturating the OPCPA stages permits amplification of pulses with nearly 80 nm bandwidth and an ~65 fs Fourier limit. As idler absorption increases above 3.4 μm in KTP, we can achieve higher output powers when tuning the signal center wavelength above 1.55 μm. The booster-amplification stages inherit the excellent short-term CEP stability from the front end [13], since the amplified spontaneous emission (ASE) is well-suppressed in our IR OPCPA. Furthermore, CEP noise from amplitude-to-phase-noise conversion from the Nd:YAG pump due to cross-phase modulation [13] is completely negligible ($<2.2\times10^{-3}\pi$). The SHG–frequency-resolved optical gating (FROG) characterization data of 3.5 mJ, 1.57 μm pulses with 62 nm bandwidth from the 20 Hz four-stage IR OPCPA (Fig. 3) indicate a 74.4 fs FWHM pulse duration, which is close to the transform limit (TL) of 72.6 fs.

To explore a possible route toward a terawatt-peak-power single-cycle IR source, we demonstrate spectral broadening of the 74.4 fs 1.57 μm pulses by filamentation in noble gases. As shown in Fig. 1, the pulses were focused using a 50 cm lens placed 4 cm in front of the AR-coated input window W1 of a 138 cm long gas cell filled with argon ($I_p=15.76$ eV) at the absolute pressure of 5 bars. In the filamentation regime without plasma-induced pulse self-compression, we generated ~3 mJ, 600-nm-wide IR supercontinua (not shown) of high spatial quality supporting 8 fs pulse durations, i.e., less than two optical cycles at 1.5 μm. Careful SHG–FROG characterization of these pulses has revealed a complex temporal structure consisting of a 200 fs FWHM main split pulse and additional low-intensity satellites. The temporal splitting apparently helps to keep the pulse intensity below the break-up threshold of a single filament. By lowering the input pulse energy and tuning the gas pressure in the cell, we achieved the regime of pulse self-compression, in which CEP-stable 2.2 mJ, 74.4 fs, 1.57 μm input pulses are compressed in a single filament in argon down to a 19.8 fs duration. The output energy was 1.5 mJ, corresponding to an energy throughput of 66%, includ-

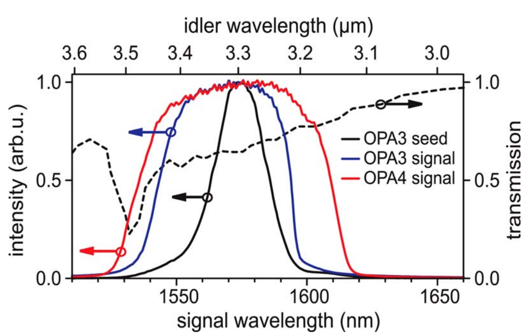

Fig. 2. (Color online) Spectral properties of the power-amplification OPCPA stages: spectrum of the third-stage seed, amplified signal spectra after stages three and four. The amount of ASE is immeasurable in the absence of the WL seed in OPA stage 1. The dashed curve indicates the idler transmission through 10 mm of KTP.

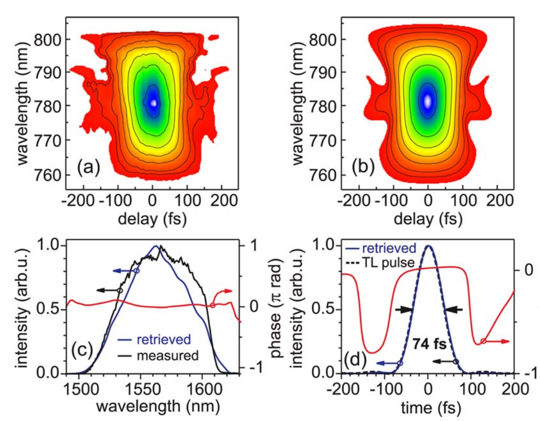

Fig. 3. (Color online) SHG–FROG characterization of the 20 Hz output from the four-stage IR OPCPA. (a) Measured and (b) retrieved FROG traces. (c) Measured spectrum, retrieved spectral intensity and phase. (d) Retrieved temporal intensity and phase profiles exhibiting a 74.4 fs FWHM pulse duration. The TL intensity profile (dashed curve) corresponds to a 72.6 fs duration.

ing the 8% reflection losses on the uncoated 1-mm-thick BK7 output window W2. A detailed study of the transition between the two distinct IR filamentation regimes, with and without self-compression, and of the CEP stability will be presented elsewhere.

The self-compression results are summarized in Fig. 4. We emphasize that the FROG characterization and output pulse energy measurement were performed without aperturing the filamentation output beam. For these experimental conditions, a supercontinuum with a 130 nm FWHM bandwidth originated from a 12–15-cm-long filament visible with the naked eye. The measured duration of the self-compressed pulse was 19.8 fs, corresponding to four cycles at 1.5 μm. This represents a temporal compression of the input pulses by a factor of ~4. Importantly, for self-compression of 2 μm pulses, Bergé [12] pointed out that, as the result of nonlinear propagation, the shortest achievable pulse duration survives only over a shorter distance of ~15–20 cm in the gas medium in comparison with the 800 nm case. Therefore, careful optimization of the propagation distance in the pressurized Ar cell behind the filament might lead to the observation of even shorter pulse durations. In addition, the spectral phase was shown to be remarkably reproducible on a daily basis, which holds potential for further recompression using chirped mirrors.

In conclusion, we have demonstrated a CEP-stable 1.5 μm OPCPA with pulse energies up to 12.5 mJ based on a fusion of a DPSS femtosecond Yb:KGW MOPA system and picosecond Nd:YAG solid-state technology. Furthermore, we demonstrated self-compression of CEP-stable 2.2 mJ, 74.4 fs, 1.57 μm input pulses down to 19.8 fs duration in a single filament in argon with 1.5 mJ output energy and a 66% energy throughput. The output energy was scaled up by 5.6 times over earlier results [11]. The output energy and energy throughput can be further increased by replacing window W2 with an AR-coated window and by systematically optimizing the experimental conditions (input pulse energy and beam diameter, focusing lens and position, gas type and pressure, and cell length). Ultimately, with our 1.6 μm pulses we expect to surpass the current energy limitation (4–5 mJ at 0.8 μm [15,16]) for gas-broadening schemes [12].

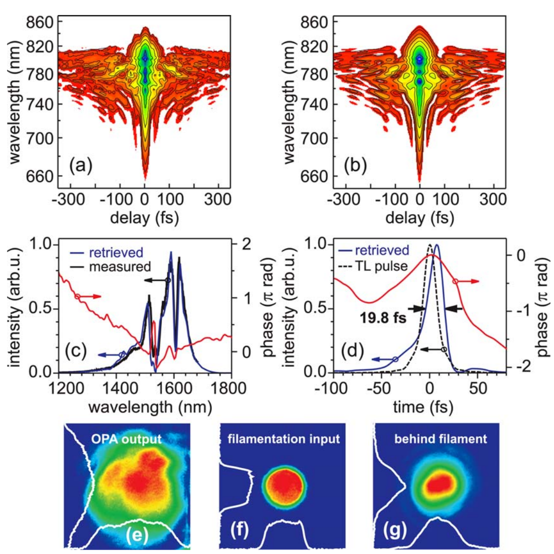

Fig. 4. (Color online) Self-compression of 1.5 mJ pulses in argon at 5 bars: (a)–(d) as in Fig. 3; retrieved pulse duration 19.8 fs, TL 15.9 fs. (e)–(g) Far-field spatial beam profiles measured with the pyroelectric 2D array: (e) after OPCPA grating compressor, (f) apertured filamentation input measured behind iris aperture A, (g) total beam profile behind the filamentation cell. Image size is 12.4 mm $\times$12.4 mm.

This research was supported by the Austrian Science Fund (FWF), grants U33-N16 and F1619-N08, LASERLAB-EUROPE II (JRA HAPPIE), and partly supported by the Lithuanian State Science and Studies Foundation, project B-42/2009. O. D. Mücke gratefully acknowledges support from a Lise-Meitner Fellowship from the FWF, project M1094-N14.

References

1. F. Krausz and M. Ivanov, Rev. Mod. Phys. **81**, 163 (2009).
2. X. Gu, G. Marcus, Y. Deng, T. Metzger, C. Teisset, N. Ishii, T. Fuji, A. Baltuska, R. Butkus, V. Pervak, H. Ishizuki, T. Taira, T. Kobayashi, R. Kienberger, and F. Krausz, Opt. Express **17**, 62 (2009).
3. C. Vozzi, F. Calegari, E. Benedetti, S. Gasilov, G. Sansone, G. Cerullo, M. Nisoli, S. De Silvestri, and S. Stagira, Opt. Lett. **32**, 2957 (2007).
4. E. J. Takahashi, T. Kanai, Y. Nabekawa, and K. Midorikawa, Appl. Phys. Lett. **93**, 041111 (2008).
5. B. Shan and Z. Chang, Phys. Rev. A **65**, 011804(R) (2001).
6. J. Tate, T. Auguste, H. G. Muller, P. Salières, P. Agostini, and L. F. DiMauro, Phys. Rev. Lett. **98**, 013901 (2007).
7. P. Colosimo, G. Doumy, C. I. Blaga, J. Wheeler, C. Hauri, F. Catoire, J. Tate, R. Chirla, A. M. March, G. G. Paulus, H. G. Muller, P. Agostini, and L. F. DiMauro, Nat. Phys. **4**, 386 (2008).
8. V. S. Yakovlev, M. Ivanov, and F. Krausz, Opt. Express **15**, 15351 (2007).
9. T. Popmintchev, M.-C. Chen, A. Bahabad, M. Gerrity, P. Sidorenko, O. Cohen, I. P. Christov, M. M. Murnane, and H. C. Kapteyn, Proc. Natl. Acad. Sci. USA **106**, 10516 (2009).
10. E. J. Takahashi, T. Kanai, K. L. Ishikawa, Y. Nabekawa, and K. Midorikawa, Phys. Rev. Lett. **101**, 253901 (2008).
11. C. P. Hauri, R. B. Lopez-Martens, C. I. Blaga, K. D. Schultz, J. Cryan, R. Chirla, P. Colosimo, G. Doumy, A. M. March, C. Roedig, E. Sistrunk, J. Tate, J. Wheeler, L. F. DiMauro, and E. P. Power, Opt. Lett. **32**, 868 (2007).
12. L. Bergé, Opt. Express **16**, 21529 (2008).
13. O. D. Mücke, D. Sidorov, P. Dombi, A. Pugžlys, A. Baltuška, S. Ališauskas, V. Smilgevičius, J. Pocius, L. Giniūnas, R. Danielius, and N. Forget, Opt. Lett. **34**, 118 (2009).
14. D. Kraemer, M. L. Cowan, R. Hua, K. Franjic, and R. J. D. Miller, J. Opt. Soc. Am. B **24**, 813 (2007).
15. A. Suda, M. Hatayama, K. Nagasaka, and K. Midorikawa, Appl. Phys. Lett. **86**, 111116 (2005).
16. G. Stibenz, N. Zhavoronkov, and G. Steinmeyer, Opt. Lett. **31**, 274 (2006).